Scanning Polarization Force Microscopy Study of the Condensation and Wetting Properties of Glycerol on Mica

Lei Xu and Miquel Salmeron*

Materials Science Division, Lawrence Berkeley National Laboratory, University of California, Berkeley, California 94720

Received: April 13, 1998; In Final Form: June 23, 1998

The condensation of glycerol on mica surfaces in ambient air was studied with scanning polarization force microscopy (SPFM). Two different wetting regimes were found that depend on the state of the surface. On freshly cleaved mica, glycerol condenses, forming flat films. The films expand until a uniform layer is formed. The first molecular layer of glycerol was found to be more strongly bound to the surface than were subsequent layers. On contaminated mica (after 2 h of exposure to air) droplets in the shape of spherical caps form that partially wet the substrate. The droplets grow indefinitely in the saturated vapor. The contact angle of droplets with heights <20 nm was found to deviate from the macroscopic value found in large drops. The results are discussed in the context of the long-range forces in the liquid film.

Introduction

Glycerol is an important liquid in many practical applications such as in cosmetology. It forms strong H-bonds and is highly viscous. Numerous studies have been conducted on its structure,[1] dielectric properties,[2] and dependence of hydrogen bonding on pressure.[3] Kane and El-Shall[4] studied the condensation of glycerol from its supersaturated vapor. However, the nanometer-scale details of the condensation of glycerol from its vapor onto a surface have not been studied because of the lack of appropriate techniques, especially in the submicrometer-scale regime, which is below the limit of optical microscopy.

Recently, scanning polarization force microscopy (SPFM) has proven to be a powerful technique to image liquid surfaces with minimal perturbation.[5] Recent studies with this technique include the deposition of water on mica,[6] the corrosion of aluminum surfaces,[7] and the adsorption of water on NaCl.[8] A review also was published recently.[9]

SPFM is based on the use of electrical forces between the tip and surface to perform noncontact imaging in an atomic force microscope (AFM) apparatus. A conductive tip biased to a few volts is used. When the tip approaches to ∼10 nm from the sample, the attractive electrostatic polarization force is kept constant by feedback control while the sample is scanned to produce constant-force images. As a result, topography, as well as surface potential and dielectric constant distribution, are recorded in the images. The contribution from surface potential variations can readily be determined from images with reverse bias, in which the area with higher surface potential appears higher with negatively biased tips and lower with positively biased tips. If the surface potential is uniform, the polarization force is sensitive to variations of the dielectric constant ϵ, but this effect is only important for materials with low values of ϵ. For large values of ϵ, the response tends to saturate because of the $(\epsilon-1)/(\epsilon+1)$ dependence of the force. Pure glycerol has a value of $\epsilon = 40$, and water−glycerol mixtures have intermediate values between this and the water value of 80. The mica substrate, when wet, also has a large dielectric constant at low frequencies, because of the mobile ions. Therefore, the contrast in the images presented here is due mostly to surface topography.

In this paper, the SPFM technique is applied to investigate the condensation of glycerol from its vapor onto mica surfaces in standard laboratory air. We show how condensation takes place under different conditions and study the wetting properties of the films and droplets formed.

Experimental Section

The SPFM setup is housed in a humidity-controlled chamber. Humidity can be reduced by flowing dry nitrogen through the chamber, or increased by vaporizing deionized water. Relative humidity (RH) is measured with an RH-20C Omega hygrometer. Most of our experiments were carried out at ∼50% RH and 21 °C.

We used silicon nitride cantilevers from Digital Instruments with a nominal spring constant of 0.58 N/m. The tip and lever were coated with a 50 nm thick layer of Pt to make them conductive. Direct current (dc) bias is usually used in this study with voltages of +6 or −6 V. The feedback controller was from RHK Technology.

The sample, consisting of a piece of muscovite mica with a diameter of ∼1 cm and thickness of ∼0.1 or 0.2 mm was glued onto a holder and mounted on the scanner of the SPFM. A reservoir of glycerol was positioned within a few centimeters from the mica substrate to produce glycerol vapor. Because of the 50% RH, the condensed film should have the corresponding equilibrium composition of water and glycerol. For simplicity, however, we will refer to the film simply as glycerol.

To follow the process of condensation, SPFM images were taken immediately after exposure of the mica to glycerol vapor. Although both positive and negative images were acquired alternatively, only the negative images are shown here. Any effect of bias sign will be discussed.

To heat the sample holder, a resistor (60 Ω, 0.125 W) was attached to it. A commercial temperature controller was used to fix the temperature of the sample with the help of a sensor. The accuracy of the temperature adjustment was ∼±0.5 °C.

S1089-5647(98)01834-3 CCC: $15.00 © 1998 American Chemical Society
Published on Web 08/21/1998

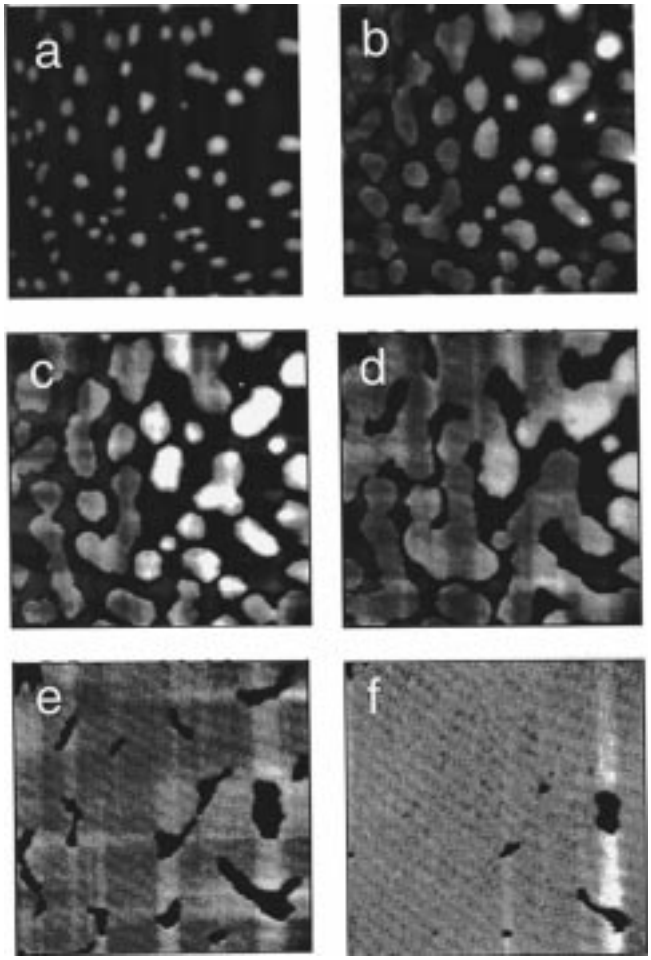

Figure 1. SPFM images (18 × 18 μm) showing the evolution of the structures formed by condensation of glycerol from its vapor on a surface of freshly cleaved mica. During imaging, the tip is biased to −6 V and scans at ∼10 nm from the sample surface. Droplets with more or less flat tops grow until their heights reach ∼10 nm. They then expand laterally and coalesce, forming flat films. The height of these films decreases slowly down to ∼3 nm just before closure of the film in (f). Notice the somewhat rounded polygonal shape of the perimeters. Experiments were performed under normal ambient conditions of 50% RH and 21 °C.

Results

Condensation on Freshly Cleaved Mica. The time evolution of the surface structure following glycerol condensation on freshly cleaved mica is illustrated by the sequence of images in Figure 1. Condensation begins with the formation of droplets (Figure 1a). These droplets could be easily wiped away by the tip if contact images are taken. The shapes of these droplets are not spherical, but resemble ellipsoids with their shorter axis in the vertical direction. As more glycerol condenses on the surface, the droplets first grow vertically and laterally. However, when their heights reach ∼10 nm, they spread and become patches with flat tops. From that point, the height of the droplets or patches decreases as they expand laterally. This evolution is shown in the profiles of Figure 2, which correspond to one of the droplets in Figure 1. Just before the film completely covers the mica surface, the relative contrast is 3 nm. Interestingly, the edges of the patches tend to have a polygonal shape, which might indicate that glycerol maintains an epitaxial relationship with the mica substrate. Under the present conditions, it took about 30 min before the whole mica surface was uniformly covered. After that, no further contrast changes could be observed in the SPFM images.

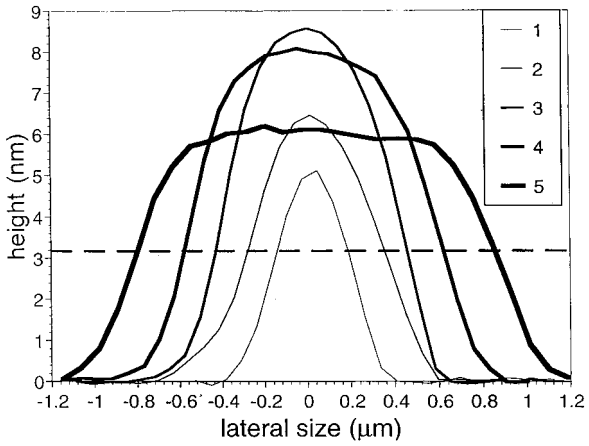

Figure 2. Profile of one droplet in Figure 1, illustrating the initial growth and the flattening that occurred, in this particular case, after a maximum height of 8.5 nm was reached. The numbers indicate the time sequence during condensation. The dashed line shows the thickness of the film after it covers most of the surface.

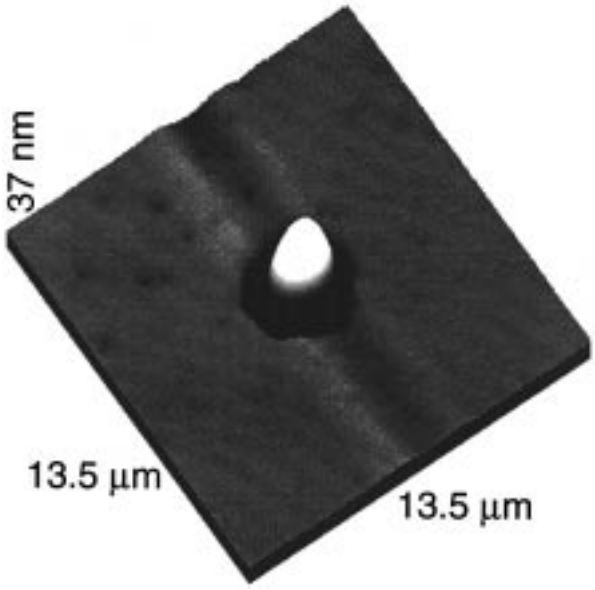

Figure 3. Structure of the liquid glycerol film on mica after disruption by a short (1 s) contact with the tip. A droplet of glycerol 30 nm high was produced that was surrounded by a region depleted of liquid. The depth of this region was ∼6 nm. Notice the polygonal shape of the empty region. The evacuated area around the droplet suggests that the liquid in the droplet was pulled from the film through capillary action rather than from the vapor phase. The droplet spreads slowly and refills the hole after some time. Image size is 13.5 × 13.5 μm.

The film uniformity can be disturbed by mechanical contact with the tip. Figure 3 shows a droplet produced by a 1-s contact with the tip after the completion of coverage in the experiment shown in Figure 1. Around the droplet, a region depleted of glycerol can be observed with a depth of 6 nm. The depleted area also has a polygonal edge. Because the depth of the depleted area in Figure 3 is larger than the thickness of the film in Figure 1f, it is clear that the condensation did not stop after uniformity was reached. The depleted area suggests that the droplet is formed by glycerol pulled out from the film to form a capillary neck around the tip, instead of direct deposition from the tip or condensation from the gas phase. The height of the droplet is ∼30 nm. The droplet slowly spreads back to refill the evacuated area and finally joins the edges of the film.

The glycerol film evaporates almost completely if the temperature of the mica is increased. We found that heating

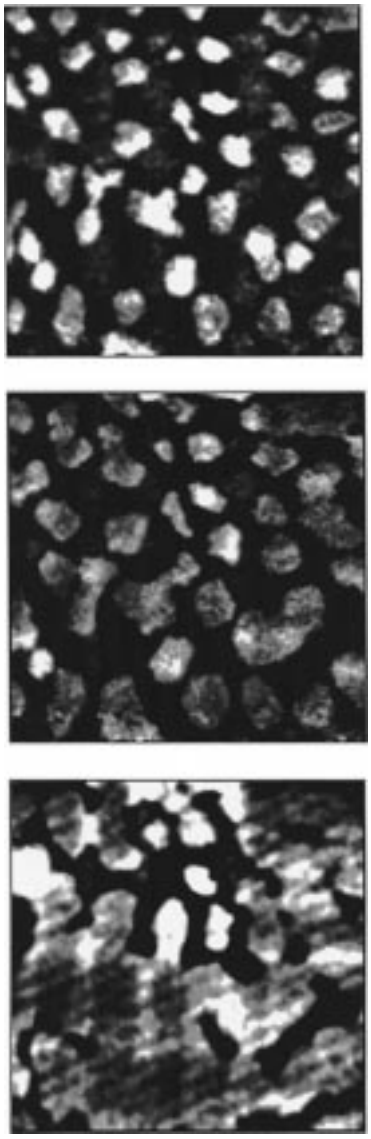

Figure 4. Structures formed by the condensation of glycerol on mica heated by 2 °C to evaporate a previously existing glycerol film. After the sample was cooled to room temperature, growth of a 1.5 nm thin two-dimensional film was observed. Image size is 18 × 18 μm.

by only 2 °C causes the glycerol to evaporate. Evaporation proceeds by retraction of the film edges, and in about 3 min, no contrast could be seen on the surface, indicating that the evaporation process is complete. If the temperature is lowered back to room temperature while glycerol vapor is still present, condensation takes place again. Figure 4 shows that this second condensation at room temperature proceeds once again in a two-dimensional manner. It starts with the formation of flat patches with an average thickness of ~1.5 nm. These patches increase in size until the layer is completed. The growth processes appear to be different in the first and second condensation experiments. The difference in measured film thickness between Figure 1f (3 nm) and Figure 4 (1.5 nm) suggests that a layer of glycerol remained on the surface that did not evaporate during the heating process. Because the condensation of glycerol takes place over a layer of the same material, a smooth layer-by-layer growth dominates the process.

To further verify this hypothesis, glycerol droplets were deposited on freshly cleaved mica in the absence of glycerol vapor. To accomplish this, the AFM tip is used as a pen to deposit glycerol by first dipping it into bulk liquid glycerol.

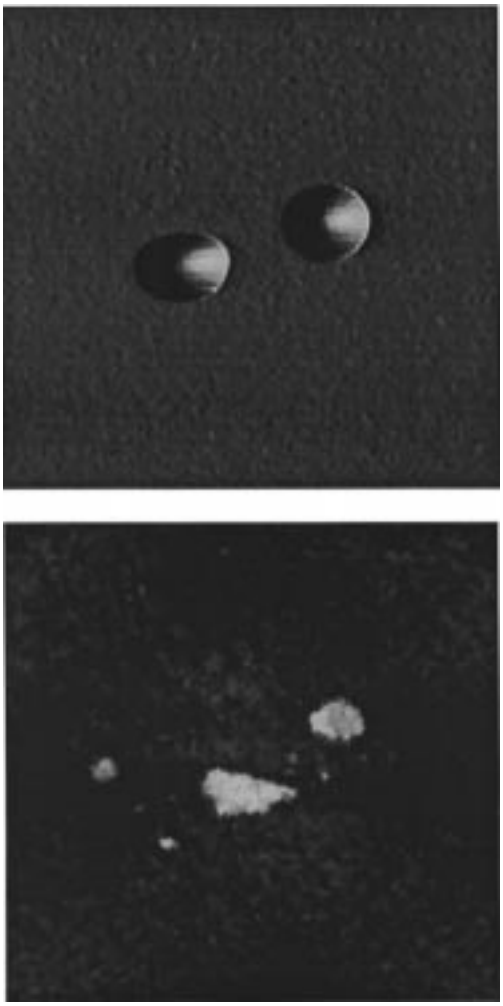

Figure 5. (a, top) Two droplets of glycerol deposited by contact with the tip. The tip in this experiment was dipped into bulk glycerol just before the deposition. (b, bottom) After the sample was heated by 2 °C, a thin layer of glycerol remained near the parent drops. This indicates that the first layer of glycerol is strongly bound to mica. Image size is 10 × 10 μm.

This is quite different from the previous contact experiment in which the material to form the droplet was pulled away from the existing film. The amount of glycerol on the tip is sufficient to deposit many drops, although with successive contacts the size of droplets decreased until the tip finally became depleted of glycerol. Figure 5a shows an image of two droplets deposited by two contacts with the glycerol-coated tip. The evaporation is slow enough that the droplets are stable on the surface for many minutes. As in the previous case, evaporation occurred readily when the sample was heated by ~2 °C. After evaporation, we found that a thin flat layer remained on the surface (Figure 5b).

In all of the images presented above, no dependence on the sign of the tip bias was observed, except for the strongly bound layers left after evaporation. When we studied the appearance of such layers, such as those in Figure 5b, under different bias polarity, we found that the layer appears lower than the surrounding area if the tip is positively biased, and higher if the tip is negatively biased. This indicates that this area has a higher surface potential than the surrounding area. Interestingly, when we reduced the RH from the ambient 50% down to ~5%, the layer appears higher in positive-bias image and lower in negative-bias image, which indicates that under dry conditions its surface potential is lower. This result can be interpreted in

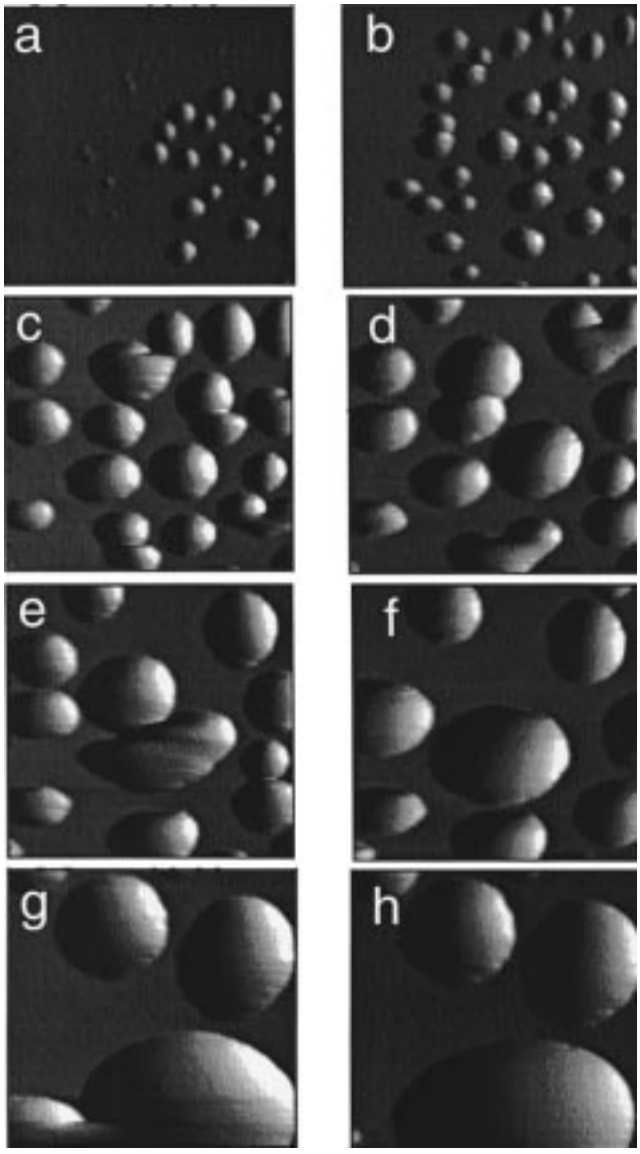

Figure 6. (a)−(h) SPFM images (18 × 18 μm) showing the condensation of glycerol on contaminated mica. The droplets increase in size while maintaining a nearly spherical cap shape. When two drops contact each other, they coalesce into a larger drop.

two ways: (a) there is some net dipole orientation of the glycerol or water molecules in the first strongly bound layer, which might depend on the amount of water in the glycerol; and (b) the potential of the mica substrate surrounding the glycerol patch changes its surface potential because of the adsorption of water. For now, we have not pursued in more detail the study of these effects as a function of humidity.

Condensation on Contaminated Mica. We also studied the condensation of glycerol on a mica surface that was exposed to air for a few hours. We shall refer to this mica surface as "contaminated" mica. We found that, in this case, glycerol does not completely wet the surface. This behavior is similar to that of water, as we have shown in a previous study. The contact angle of water on mica surfaces increased from 0° on the freshly cleaved surface to a small value between 2 and 3° on the contaminated mica.[6]

On this slightly hydrophobic surface, the condensed glycerol nucleates into droplets that grow with time, as shown in the sequence of images in Figure 6. This behavior is in sharp contrast to the case of freshly cleaved mica. The droplet shape is very close to a spherical-cap, as shown by the linear correlation coefficient of 0.991 found from a fit to a sphere. When two droplets grow close enough to each other, they coalesce, as can be seen in several images in Figure 6. The droplets never flatten out, but continue to grow as spherical-cap shapes, even when the lateral diameter is >15 μm, the largest dimension of our images.

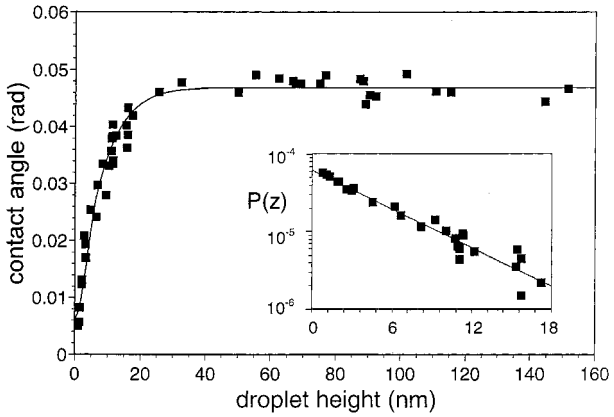

Figure 7. Plot of the contact angle θ of the drops formed by condensation of glycerol on contaminated mica vs drop height e. A rapid increase occurs up to 20 nm (corresponding to a drop with a base diameter of ∼2.2 μm), where it reaches a constant value θ_0. Inset: Plot of $[\theta_0^2 - \theta^2]/(1 + e/\delta)$ vs e. This plot shows that the potential due to the long-range forces depends exponentially on the distance (see text).

The height of the droplets is in the nanometer range, where surface forces could affect the contact angle θ and cause it to depart from the macroscopic value θ_o. We thus measured θ as a function of drop height. We indeed found that θ deviates from the value for large drops when the droplet height is < ∼20 nm. The value of θ is determined from the measured height e and the basal radius r of the droplets, using the expression $\theta = 2e/r$.

The results from measurements of many droplets are shown in Figure 7. As we show in the discussion, this curve can be explained by the effect of long-range forces, as predicted from wetting theories.

Discussion

Effect of Long-Range Forces in the Geometric Structure of the Liquid Film. To analyze the shape of glycerol films and droplets, we followed the work of de Gennes and co-workers[10−12] on the effect of long-range forces on the structure and wetting properties of liquid films. The shape $z(r)$ of a liquid drop on a solid surface can be obtained from the minimization of the free energy. For a circularly symmetric drop, this energy can be written as an integral over the area covered by the drop:

$$G = G_0 + \int_{drop} 2\pi r\, dr\left[-S + \frac{\gamma}{2}\left(\frac{dz}{dr}\right)^2 + P(z) - \frac{\mu_{vapor} - \mu_{liq}}{v_{mol}}\cdot z\right] \quad (1)$$

where $S = \gamma_{sv} - \gamma_{sl} - \gamma$ is the spreading coefficient and γ_{sv}, γ_{sl}, and γ are the solid−vapor, solid−liquid, and liquid−vapor surface energies, respectively. The second term is due to the excess surface because of the curvature of the drop and is valid for shallow drops where $dz/dr \ll 1$. The third term is the potential energy between the surfaces (from which the disjoining pressure originates). The last term describes the supersaturation in terms of the chemical potentials of the vapor and the liquid.

v_{mol} is the molecular volume. The minimization of eq 1 under constant volume gives the condition:

$$P'(z) - \lambda = \gamma \cdot z'' + \gamma \cdot \frac{z'}{r} \tag{2}$$

which has a first integral of the form:

$$P(z) - P(e) - \lambda \cdot (z - e) = \frac{1}{2}\gamma \cdot z'^2 + \gamma \cdot \int_e^z \frac{z'^2}{r} dr \tag{3}$$

where λ is a Lagrange multiplier that includes the supersaturation term, and e is the droplet height. The prime symbols denote derivatives with respect to z or r. This equation can be used, together with the experimental profile of the drop, for a direct determination of $P(z)$. The multiplier λ can be found from the drop volume. The method was used recently to analyze the contact angle of microscopic droplets of sulfuric acid on mica.[13] In the present work, however, we use another method based on an approximate integration of eq 3 that allows us (under certain conditions) to ignore the precise details of the shape of the drop.

For flat films, the minimization of the free energy gives the following relation between the potential P and its derivative or disjoining pressure Π ($\Pi \equiv -dP/dz$):

$$S = P(e) + e \cdot \Pi(e) \tag{4}$$

where e is the thickness of the film.

Contaminated Mica. We have seen that on contaminated mica glycerol does not wet the surface ($S < 0$) and forms droplets with shapes very close to spherical caps. This fact can be used to obtain an approximate solution of the integral in eq 3. If R is the radius of the spherical drop, then from eq 2 we find that $\lambda = 2/R + P'(e)$. The integral in eq 3 can be performed assuming a spherical shape, which is a very good approximation, particularly around the top of the drop. The result is:

$$P(z) - P(e) - \left[\frac{\gamma}{R} + P'(e)\right](z - e) = \frac{\gamma}{2} \cdot z'^2$$

In our case, this formula should be a good approximation down to near the base of the drop. For $z \rightarrow 0$, this expression can be written in the more convenient form:

$$\theta^2 = \theta_0^2 + \frac{2}{\gamma} \cdot [P(e) + e \cdot \Pi(e)] \tag{5}$$

where $\theta_0^2 = -(2/\gamma) \cdot P(0)$ is the asymptotic (macroscopic) value of the contact angle squared. $P(0)$ is the spreading coefficient S. The slope of the droplet at its baseline is determined by the envelope of molecular layers of glycerol and water molecules near the edge of the drop and is assumed to be much smaller than either θ or θ_0.

The observed decrease of contact angle as the droplet height decreases indicates that the potential $P(e)$ is negative. We can use eq 5 together with the data in Figure 7 to explore the type of potential P that governs the glycerol−hydrophobic mica interaction. We considered inverse power law functions ($P \sim -A/z^n$) and exponential functions $P \sim -P_0 \cdot \exp(-z/\delta)$. Only the exponential dependence gives a good fit, as shown in the inset of Figure 7, a semilog plot of $P(e)$ vs e. The fitting parameters were $\delta = 5$ nm and the strength of the potential at $e = 0$ (i.e., the spreading coefficient) is $S = -6.4 \times 10^{-5}$ J·m^{-2}. This gives a value for the negative disjoining pressure of ~1 atm. The observed exponential dependence might be indicative of structural or hydrophobic attractive forces between the glycerol−air interface and the glycerol−mica interface. These forces appear to be a factor of 100 lower than typical values for water between hydrophobic surfaces,[14] which might be explained by the low hydrophobicity of our contaminated mica.

Hydrophilic Mica. For the case of glycerol condensing on freshly cleaved mica that is hydrophilic, S should be positive. As we have seen, as the drops form, they first grow until a maximum height of ~10 nm at which they flatten out and increase in lateral size. Formation of flat pancakes is predicted in the complete wetting situation in the case of $S > 0$ and repulsive potential (positive disjoining pressure), as described by Brochard-Wyart et al.[12] Cazabat et al.[15] discuss various types of pancakes according to their thickness, which is a strong function of the spreading coefficient S. In the so-called "American pancakes", the thickness is several nanometers and therefore involves multimolecular layers. This appears to be the situation in our case, because the thickness is 3 nm. Unfortunately, we do not have a measure of S or of the strength of the potential for this case. In the previous section, we found that the value of S for the slightly hydrophobic mica was -6.4×10^{-5} J·m^{-2}, a value that is 3 orders of magnitude smaller than typical values of the surface tension γ of glycerol or water (6.3 and 7.3 × 10^{-2} J/m^2, respectively). The observations would be explained if the effect of the contamination was to change the sign of S without substantially altering its order of magnitude value. Conversely, the observed multimolecular thickness of the film might be taken as an indication that indeed the condition of a small S value is fulfilled in this case. The fact that the experiments are carried out in a humid environment at 50% RH, and that water wets mica in addition to being completely miscible with glycerol might play a significant role. If γ_{sv} is the surface tension of mica covered with a water layer (~73 mJ/m^2) and glycerol adsorbs with a composition changing smoothly over a few layers from water to glycerol−water, then one could indeed have $S = \gamma_{sv} - \gamma_{sl} - \gamma \approx 0$.

The initial growth of the drop and subsequent decrease in height upon flattening (Figure 2) are not expected from the wetting theories discussed above. The first droplets probably form around preexisting defects or nucleation sites that attract glycerol more strongly than mica. It is possible that this behavior also reflects an incomplete equilibrium due to the slow diffusion of condensed glycerol. We have indeed seen that holes created by disruption of the completed film refill slowly. Also, the droplet left in the center of the hole in Figure 3 is much higher (30 nm) than the equilibrium film thickness, and yet it relaxes slowly to refill the hole. Another possibility is that some weakly bound material has to be displaced first from the mica in order for glycerol to spread efficiently. This should give rise to hysteresis in the condensation dynamics and is perhaps the reason for the difference in behavior between the first and second adsorption experiments. Finally, one can also explain the observed behavior as the result of an energy per unit perimeter, or line tension.[16] For circular films, this line tension model predicts first an increase of droplet height and then a decrease as the volume increases, as was observed here, provided that the extra energy per unit length is positive. The noncircular nature of the islands in Figure 1 complicates comparison with model potentials. In fact, crystallographic effects are observed in the shape of the pancakes, which indicates a directional dependence of the line tension. The only information that can be extracted from data such as those in Figure 2 is a characteristic length, beyond which line tension effects are not important. In our case, this length is on the order of 1 μm.

Also, unlike the previous case of attractive long-range forces, in which the contact angle varied continuously with drop height and allowed us to study the functional form of $P(e)$, the formation of flat films makes accessible only one value of the potential. This corresponds to $e \sim 3$ nm, the observed asymptotic height. Because S is unknown, the value of P (3 nm) cannot be determined. This value of e should be on the order of the range of the repulsive long-range forces. A detailed analysis of the functional shape of the pancake at its borders could, in principle, be performed to obtain $P(e)$. We have not yet attempted this analysis.

The observation of a film that remains bound to the surface after evaporation indicates that the forces near the surface are strong, and that the long-range part of the potential $P(e)$ discussed above does not adequately describe the energetics of the first molecular layers. The structure of these layers is determined by the short-range part of the forces. These forces might also be responsible for the tendency of the films to adopt a polygonal structure, which probably reflects a crystalline arrangement near the interface. Also, the influence or existence of a water film on the surface might play an important role in the binding of the first layer.

Conclusions

The condensation of glycerol on freshly cleaved mica begins with the formation of droplets that grow to a limited height before spreading out into flat films that tend to have polygonal shapes. These results indicate a small but positive spreading coefficient combined with the action of repulsive long-range forces (positive disjoining pressure). At short range, the surface forces give rise to a strong binding of the bottom layer of condensed glycerol.

On mica rendered hydrophobic by contamination, glycerol forms droplets with shapes similar to spherical caps. The contact angle of the droplets increases with height up to ~20 nm, and then remains constant. This can be explained by the combined action of attractive long-range forces, which produces a negative disjoining pressure, and a negative spreading coefficient.

We have shown how the contact angle can be correlated in a simple way to the potential due to long-range surface forces in the case of nearly spherical drops. From a fit to the experimental data, an exponential form for the long-range force was obtained. This seems to indicate that the force originates from hydrophobic interactions.

Our results demonstrate that the SPFM technique is very useful in studies of the structure of liquid films in the nanometer range, where long-range forces play an important role.

Acknowledgment. This work was supported by the Lawrence Berkeley National Laboratory through the Director, Office of Energy Research, Basic Energy Science, Materials Science Division of the U.S. Department of Energy under contract DE-AC03-76SF00098. We also thank Dr. François Rieutord for helpful discussions.

References and Notes

(1) Sarkar, S.; Joarder, R. N. *Phys. Lett. A* **1996**, *222*, 195.
(2) Paluch, M.; Rzoska, S. J.; Habdas, P.; Ziolo, J. *J. Phys.* **1996**, *8*, 10885.
(3) Root, L. J.; Berne, B. J. *J. Chem. Phys.* **1997**, *107*, 4350.
(4) Kane, D.; El-Shall, M. S. *J. Chem. Phys.* **1996**, *105*, 7617.
(5) Hu, J.; Xiao, X. D.; Salmeron, M. *Appl. Phys. Lett.* **1995**, *67*, 476.
(6) Xu, L.; Lio, A.; Hu, J.; Ogletree, D. F.; Salmeron, M. *J. Phys. Chem. B* **1998**, *102*, 540.
(7) Dai, Q.; Hu, J.; Freedman, A.; Robinson, G. N.; Salmeron, M. *J. Phys. Chem.* **1996**, *100*, 9.
(8) Dai, Q.; Hu, J.; Salmeron, M. *J. Phys. Chem. B* **1997**, *101*, 1994.
(9) Salmeron, M.; Xu, L.; Hu, J.; Dai, Q. *MRS Bull.* **1997**, *22*, 36.
(10) de Gennes, P.-G. *Rev. Mod. Phys.* **1985**, *57*, 827.
(11) Joanny, J. F.; de Gennes, P.-G. *J. Colloid Interface Sci.* **1986**, *111*, 94.
(12) Brochard-Wyart, F.; di Meglio, J.-M.; Quere, D.; de Gennes, P.-G. *Langmuir* **1991**, *7*, 335.
(13) Rieutord, F.; Salmeron, M. *J. Phys. Chem. B* **1998**, *102*, 3941.
(14) Israelachvili, J. *Intermolecular and Surface Forces*, 2nd ed.; Academic Press: San Diego, 1997; p 284.
(15) Cazabat, A. M.; Fraysse, N.; Heslot, F.; Levinson, P.; Marsh, J.; Tiberg, F.; Valignat, M. P. *Adv. Colloid Interface Sci.* **1994**, *48*, 1.
(16) The line tension we consider here is not the same as that in ref. 11, by J. F. Joanny and P. G. de Gennes. These authors showed that the effect of long-range forces is formally equivalent to a line tension. In our case, we introduce an additional energy term due to the lower coordination of molecules at step edges present in the perimeter of the drop.